



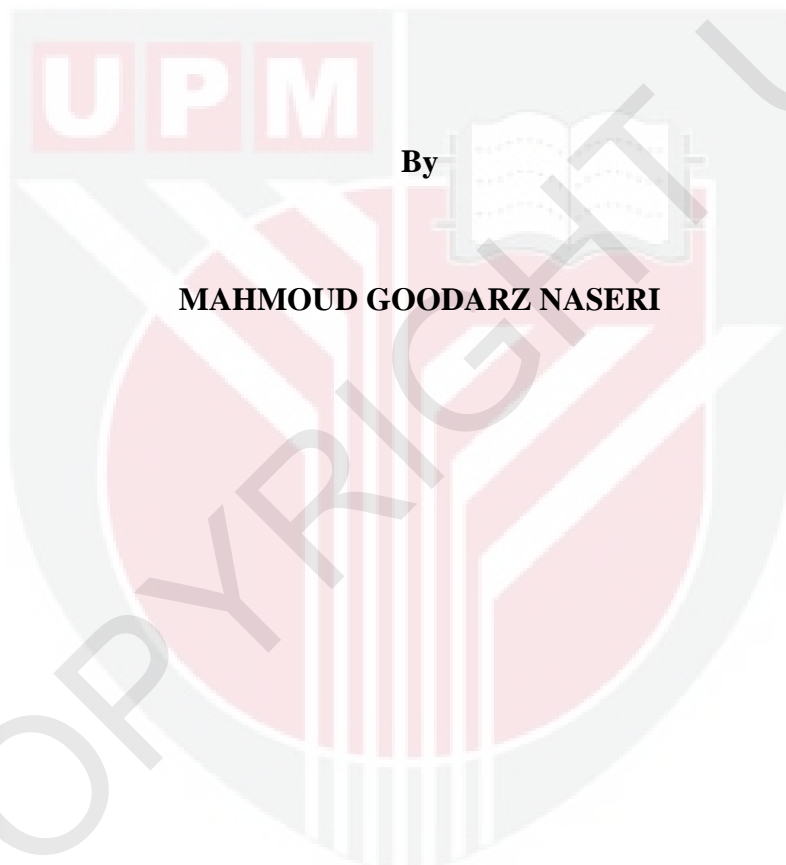
**UNIVERSITI PUTRA MALAYSIA**

***SYNTHESIS AND CHARACTERIZATION OF STRUCTURE AND MAGNETIC  
PROPERTIES OF FERRITE NANOPARTICLES PREPARED BY THERMAL  
TREATMENT METHOD***

**MAHMOUD GOODARZ NASERI**

**FS 2012 16**

**SYNTHESIS AND CHARACTERIZATION OF STRUCTURE AND  
MAGNETIC PROPERTIES OF FERRITE NANOPARTICLES PREPARED  
BY THERMAL TREATMENT METHOD**



**Thesis Submitted to the School of Graduate Studies, Universiti Putra  
Malaysia, in Fulfilment of the Requirements for the Degree of Doctor of  
Philosophy**

**February 2012**



**DEDICATED TO MY WIFE**

Abstract of the thesis presented to the Senate of Universiti Putra Malaysia in  
fulfillment of requirement for the degree of Doctor of Philosophy

**SYNTHESIS AND CHARACTERIZATION OF STRUCTURE AND  
MAGNETIC PROPERTIES OF FERRITE NANOPARTICLES PREPARED  
BY THERMAL TREATMENT METHOD**

**By**

**MAHMOUD GOODARZ NASERI**

**February 2012**

**Chairman:** **Professor Elias Saion, PhD**

**Faculty:** **Science**

Spinel ferrite nanocrystals are regarded as one of the most important inorganic nanomaterials because of their electronic, optical, electrical, magnetic, and catalytic properties. These properties are dependent on the chemical composition and microstructural characteristics in which the particle size and shape might be controlled in the fabrication processes. The preparation of spinel ferrite nanocrystals through different routes has become an essential in research and development. But, the most commonly applied synthesis methods are difficult to employ on a large scale because of their complicated procedures, high reaction temperatures, long reaction times, toxic reagents and by-products, and their potential harm to the environment. In this thesis a simple thermal treatment method is described for synthesis of spinel ferrite  $MFe_2O_4$  ( $M = Ni, Co, Mn, Zn$ , or their binary metal) nanoparticles. In this method, an aqueous solution of poly (vinyl pyrrolidone) (PVP)

was prepared by dissolving the polymer in deionized water at 343 K before adding iron nitrate and respective metal nitrates and constantly stirring at 353 K for 2 h. The dissolved solution was heated until dried at 353 K for 24 h on a glass Petri dish. The solid and orange coloured transparent remains were crushed and ground in a mortar to form powder before calcinations at different temperatures for 3 h to decompose organic matters and crystallized the ferrite nanoparticles. We concluded that the effect and role of PVP in the synthesis of cobalt ferrite nanoparticles by the thermal treatment method is astonishing. Briefly, as was discussed when we considered our XRD results, TEM images, and FT-IR spectra, PVP plays four crucial roles in synthesizing cobalt ferrite nanoparticles, i.e., (1) the control of the growth of the nanoparticles by varying the concentration of PVP; (2) the prevention of agglomeration of the nanoparticles; (3) the enhancement of the degree of the crystallinity of the nanoparticles, and (4) the production of nanoparticles that have a uniform distribution of shapes. Thermo-gravimetry analyses was used to estimate a range of calcination temperature where the polymer mass loss started at 678 K and has the maximum decomposition at 778 K. The optimum calcination temperature was confirmed by Fourier transform infrared spectroscopy (FTIR) measurement by the presence of metal oxide bands at all temperatures and the absence of organic bands at 723 and 823 K for  $\text{NiFe}_2\text{O}_4$  and  $\text{CoFe}_2\text{O}_4$  nanoparticles and at 873 K for,  $\text{MnFe}_2\text{O}_4$ ,  $\text{ZnFe}_2\text{O}_4$  and  $\text{Ni}_{x} \text{Co}_{1-x} \text{Fe}_2\text{O}_4$  nanoparticles. The transmission electron microscopy (TEM) images showed cubical spinel ferrite nanoparticles that were uniform in both morphology and particle size distribution. The x-ray diffraction (XRD) diffraction patterns showed crystalline phases that confirmed the formation of nanocrystalline single-phase spinel ferrite nanoparticles with a face-centered cubic structure, common structure for nanomaterials. The average particle sizes were

determined from TEM images and found the particle size increased with the calcinations temperature from 7 to 47 nm for NiFe<sub>2</sub>O<sub>4</sub>, from 12.5 to 39 for CoFe<sub>2</sub>O<sub>4</sub>, from 12 to 22 nm for MnFe<sub>2</sub>O<sub>4</sub>, from 17 to 31 nm for ZnFe<sub>2</sub>O<sub>4</sub> and from 14 to 25 nm for Ni<sub>x</sub>Co<sub>1-x</sub>Fe<sub>2</sub>O<sub>4</sub> nanoparticles. These sizes are in a good agreement with XRD results.

The magnetic properties were determined by vibrating sample magnetometer (VSM), which showed that the calcined samples exhibited ferromagnetic, ferromagnetic or superparamagnetic behaviors. The VSM results displayed ferromagnetic behaviors for NiFe<sub>2</sub>O<sub>4</sub>, CoFe<sub>2</sub>O<sub>4</sub>, and Ni<sub>x</sub>Co<sub>1-x</sub>Fe<sub>2</sub>O<sub>4</sub> nanoparticles and super paramagnetic behaviors for MnFe<sub>2</sub>O<sub>4</sub> and ZnFe<sub>2</sub>O<sub>4</sub> nanoparticles. The magnetic properties acquired by VSM, such as saturation magnetization and coercivity field are dependent on the calcination temperatures. The magnetic properties were also confirmed by the use of electron paramagnetic resonance (EPR) spectroscopy, which revealed the existence of unpaired electrons and also measured peak-to-peak line width ( $\Delta H_{pp}$ ), resonant magnetic field ( $H_r$ ), and the g-factor for MnFe<sub>2</sub>O<sub>4</sub> and ZnFe<sub>2</sub>O<sub>4</sub> nanoparticles while NiFe<sub>2</sub>O<sub>4</sub>, CoFe<sub>2</sub>O<sub>4</sub>, and Ni<sub>x</sub>Co<sub>1-x</sub>Fe<sub>2</sub>O<sub>4</sub> nanoparticles did not exhibit resonance signal. This could be possibly due to the super exchange interaction produces that occurs in these nanoparticles.

Our results show that we have succeeded in fabricating crystalline NiFe<sub>2</sub>O<sub>4</sub>, CoFe<sub>2</sub>O<sub>4</sub>, MnFe<sub>2</sub>O<sub>4</sub>, ZnFe<sub>2</sub>O<sub>4</sub> and Ni<sub>x</sub>Co<sub>1-x</sub>Fe<sub>2</sub>O<sub>4</sub> nanoparticles by a simple thermal treatment method. This method is cost-effective, environmentally-friendly, has low reaction temperatures, and produced no by-product effluents. It can be extended to fabricating other spinel ferrite nanoparticles of interest or other metallic oxides nanocrystals.

Abstrak tesis yang dikemukakan kepada Senat Universiti Putra Malaysia sebagai  
memenuhi keperluan untuk ijazah Doktor Falsafah

**SINTESIS DAN PENCIRIAN STRUKTUR DAN HARTANAH MAGNETIK  
FERIT NANOPARTIKEL DISEDIAKAN OLEH KADEAH RAWATAN  
TERM**

Oleh

**MAHMOUD GOODARZ NASERI**

February 2012

Pengerusi: **Profesor Elias Saion, PhD**

Faculti: **Sains**

Habur nano spinel ferit dianggap sebagai salah satu bahan nano bukan organik yang paling penting kerana sifat-sifat elektronik, optik, elektrik, magnetik, dan sebagai pemangkin bergantung kepada komposisi kimia dan ciri-ciri mikrostruktur di mana saiz zarah dan bentuknya mungkin boleh dikawal dalam proses fabrikasi. Penyediaan hablurnano spinel ferit melalui laluan yang berbeza telah menjadi penting dalam penyelidikan dan pembangunan. Tetapi, kaedah sintesis yang biasa digunakan adalah sukar untuk digunakan secara besar-besaran kerana kaedahnya yang rumit, suhu tindakbalas yang tinggi, masa tindakbalas panjang, reagen dan biproduk yang toksik, dan berpotensi membawa kemudarat kepada alam sekitar. Dalam tesis ini fabrikasi kaedah rawatan haba yang mudah untuk sintesis spinel ferit zarahnano  $MFe_2O_4$  ( $M = Ni, Co, Mn, Zn$ , atau binari logam mereka) diketengahkan. Dalam

kaedah ini, penyelesaian berair poli (vinil pyrrolidone) (PVP) telah disediakan dengan melarutkan polimer di dalam air takberion pada suhu 343 K sebelum menambah nitrat-nitrat ferum dan logam lain berkenaan dan sentiasa dikacau pada 353 K selama 2 jam. Kemudian larutan itu dipanaskan sehingga kering pada 353 K selama 24 jam kaca Petri. Sebatian pepejal dan berwarna oren telah dihancurkan dan dikisar menggunakan lesung kepada bentuk serbuk sebelum diapurkan pada suhu yang berbeza selama 3 jam untuk menguraikan bahan organik dan proses penghabluran zarahnano ferit. Kami menyimpulkan bahawa kesan dan peranan PVP dalam sintesis nanopartikel kobalt ferit dengan kaedah rawatan haba memerlukan. Secara ringkas, seperti yang telah dibincangkan apabila kita menganggap keputusan XRD kami, imej TEM, dan Spektrum FT-IR, PVP memainkan empat peranan penting dalam sintesis nanopartikel ferit kobalt, iaitu, (1) kawalan pertumbuhan yang nanopartikel dengan mengubah kepekatan PVP; (2) pencegahan pengaglomeratan yang nanopartikel; (3) peningkatan ijazah penghabluran yang nanopartikel, dan (4) pengeluaran nanopartikel yang mempunyai taburan seragam bentuk.

Termal-analisis gravimetri telah digunakan untuk menganggarkan julat suhu proses mengapur di mana kerugian jisim polimer bermula pada 678 K dan penguraian maksimum pada 778 K. Suhu proses mengapur optimum telah disahkan oleh pengukuran spektroskopi Fourier inframerah (FTIR) dengan kehadiran spectrum jalur oksida logam pada semua suhu dan ketiadaan spectrum jalur organik di 723 dan 823 K masing-masing untuk zarahnano  $\text{NiFe}_2\text{O}_4$  dan  $\text{CoFe}_2\text{O}_4$  dan pada 873 K untuk zarahnano  $\text{MnFe}_2\text{O}_4$ ,  $\text{ZnFe}_2\text{O}_4$  dan  $\text{Ni}_{x} \text{Co}_{1-x} \text{Fe}_2\text{O}_4$ . Imej mikroskopi elektron transmisi (TEM) menunjukkan struktur spinel ferit berkubus yang seragam dalam kedua-dua morfologi dan taburan saiz zarah. Corak pembelauan daripada pembelauan sinar-x (XRD) menunjukkan fasa hablur yang mengesahkan

pembentukan hablurnano fasa tunggal dengan struktur kubus muka berpusatkan (fcc) lazim bagi struktur bahan nano. Purata saiz zarah ditentukan dari imej TEM dan mendapati saiz zarah meningkat dengan suhu dari 7 hingga 47 nm untuk  $\text{NiFe}_2\text{O}_4$ , 12.5-39 nm untuk  $\text{CoFe}_2\text{O}_4$ , dari 12 hingga 22 nm untuk  $\text{MnFe}_2\text{O}_4$ , dari 17 hingga 31 nm untuk  $\text{ZnFe}_2\text{O}_4$  dan 14-25 nm untuk  $\text{Ni}_{x} \text{Co}_{1-x} \text{Fe}_2\text{O}_4$  nanopartikel. Saiz ini memenuhi pengukuran dengan keputusan XRD. Sifat-sifat magnet telah ditentukan oleh magnetometer sampel bergetar (VSM), yang menunjukkan bahawa sampel mempamerkan feromagnet, ciri-ciri feromagnet atau superparamagnetic. Keputusan VSM mempamirkan ciri-ciri feromagnet untuk zarahnano  $\text{NiFe}_2\text{O}_4$ ,  $\text{CoFe}_2\text{O}_4$ , dan  $\text{Ni}_{x} \text{Co}_{1-x} \text{Fe}_2\text{O}_4$  dan ciri-ciri super paramagnet untuk zarahnano  $\text{MnFe}_2\text{O}_4$  dan  $\text{ZnFe}_2\text{O}_4$ . Ciri-ciri magnet yang diperolehi oleh VSM, seperti kemagnetan tenu dan medan coercivity bergantung kepada suhu proses mengapur. Sifat-sifat magnet telah juga disahkan oleh penggunaan spektroskopi resonans paramagnet elektron (EPR), yang mendedahkan kewujudan elektron berpasangan dan juga diukur talian puncak-ke-puncak lebar ( $\Delta H_{pp}$ ), salunan medan magnet ( $H_r$ ), dan factor-g untuk zarahnano  $\text{MnFe}_2\text{O}_4$  dan  $\text{ZnFe}_2\text{O}_4$  manakala zarahnano  $\text{NiFe}_2\text{O}_4$ ,  $\text{CoFe}_2\text{O}_4$ , dan  $\text{Ni}_{x} \text{Co}_{1-x} \text{Fe}_2\text{O}_4$  tidak menunjukkan isyarat resonans. Ini mungkin disebabkan oleh interaksi pertukaran super berlaku dalam zarahnano. Keputusan kami menunjukkan bahawa kita telah berjaya dalam fabrikasi hablur zarahnano  $\text{NiFe}_2\text{O}_4$ ,  $\text{CoFe}_2\text{O}_4$ ,  $\text{MnFe}_2\text{O}_4$ ,  $\text{ZnFe}_2\text{O}_4$  dan  $\text{Ni}_{x} \text{Co}_{1-x} \text{Fe}_2\text{O}_4$  oleh kaedah rawatan kaedah haba yang mudah. Kaedah ini adalah kos efektif, mesra alam, mempunyai suhu tindak balas yang rendah, dan tidak menghasilkan produk efluen. Ia boleh diperluaskan kepada fabrikasi zarahnano spinel ferit yang berkepentingan atau fabrikasi hablurnano oksida logam lain.

## **ACKNOWLEDGEMENTS**

First and foremost, I would like to extend my deepest praise to Allah who has given me the patience, strength, determination and courage to complete this project within the allotted time frame.

It is my pleasure to acknowledge my supervisor, Prof. Dr. Elias Saion for giving me the platform to pursue my studies and to give me the opportunity to explore the insights of ferrite science. I would also like to extend my sincere appreciation to my supervision committee member Prof. Dr. Abdul Halim Shaari and Assc. Prof. Dr. Mansor Hashim who were ever willing to give their helps throughout this project.

I am sincerely thankful to my family for their love, understanding, and support. Without them, this work would not have been possible.

Lastly, I am thankful to my friends for all their feedbacks and helps during the research effort.

This thesis was submitted to the senate of Universiti Putra Malyasia and has been acceptance fulfilment of the requirement for the degree of Doctor of Philosophy. The members of the supervisory Committee were as follows:

**Elias Bin Saion , PhD**

Professor

Faculty of Science

Universiti of Putra Malaysia

(Chairman)

**Abdul Halim Shaari, PhD**

Professor

Faculty of Science

Universiti Putra Malaysia

(Member)

**Mansor Hashim, PhD**

Associate Professor

Universiti Putra Malaysia

(Member)

---

**BUJANG BIN KIM HUAT, PhD**

Professor and Dean

School of Graduate Studies

Universiti Putra Malaysia

Date: February 2012

## TABLE OF CONTENTS

	Page
<b>ABSTRACT</b>	ii
<b>ABSTRAK</b>	vv
<b>ACKNOWLEDGEMENTS</b>	v iii
<b>APPROVAL</b>	ix
<b>DECLARATION</b>	x
<b>LIST OF TABLES</b>	xvii
<b>LIST OF FIGURES</b>	xx
<b>LIST OF ABBREVIATIONS</b>	x xvii
CHAPTER	
<b>1 INTRODUCTION</b>	1
1.1 Nanoscience and Nanotechnology	1
1.2 Magnetic Metal Nanoparticles	2
1.3 Problem Statement	5
1.4 Significant of the Study	7
1.5 Objectives of the Study	9
1.6 Outline of the Thesis	9
<b>2 LITERATURE REVIEW</b>	11
2.1 Ferrite Nanoparticles	11
2.1.1 Garnets Ferrites	15
2.1.2 Hexagonal Ferrites	15
2.1.3 Cubic Ferrites	16
2.1.3.1 Normal Spinel Ferrites	19
2.1.3.2 Inversed Spinel Ferrites	19
2.1.3.3 Mixed Spinel Ferrites	20
2.2 Classification and Applications of Ferrites	21
2.3 Established Methods for Synthesis of Nanocrystalline Ferrites	26
2.3.1 Ceramic Method	27
2.3.2 Sol-gel Method	27
2.3.3 Co-precipitation Method	28
2.3.4 Hydrothermal Method	28

2.3.5	Ball Milling Method	29
2.3.6	Reverse Micelle Method	29
2.3.7	Microemulsions Method	29
<b>3</b>	<b>THEORY</b>	<b>31</b>
3.1	Theory of Magnetism	31
3.1.1	The Bohr Theory of Magnetism and Spin Moments	31
3.1.2	Magnetic Field and Magnetic Moment	33
3.1.3	Magnetic Behaviours	36
3.1.3.1	Diamagnetism	37
3.1.3.2	Paramagnetism	38
3.1.3.3	Ferromagnetism and Ferrimagnetism	39
3.1.3.4	Antiferromagnetism	40
3.1.3.5	Superparamagnetic	40
3.1.4	Domains	42
3.1.5	Magnetization Curve and Hysteresis Loops	44
3.2	Electron Paramagnetic Resonance Spectroscopy (EPR)	47
3.2.1	The Essence of EPR	47
3.2.2	The Hyperfine Interaction	49
3.2.3	The Dipole-Dipole Interaction	51
<b>4</b>	<b>METHODOLOGY AND EXPERIMENTAL</b>	<b>52</b>
4.1	Introduction	52
4.2	Thermal Treatment Method	52
4.3	Materials	54
4.4	Experimental Procedure	54
4.4.1	Process of Synthesis of Nickel Ferrite Nanoparticles	55
4.4.2	Process of Synthesis of Cobalt Ferrite Nanoparticles	55
4.4.3	Process of Synthesis of Manganese Ferrite Nanoparticles	56
4.4.4	Process of Synthesis of Zinc Ferrite Nanoparticles	57
4.4.5	Process of Synthesis of Nickel Cobalt Ferrite Nanoparticle	57
4.5	Characterization	58
4.5.1	Thermo-Gravimetry Analyses (TGA)	59

4.5.2	X-ray Diffraction (XRD)	59
4.5.3	Fourier Transform Infrared Spectroscopy (FTIR)	59
4.5.4	Transmission Electron Microscopy	59
4.5.5	Scanning Electron Microscopy (SEM)	60
4.5.6	Vibrating Sample Magnetometer (VSM)	60
4.5.7	Electron Paramagnetic Resonance (EPR)	60
<b>5</b>	<b>RESULTS AND DISCUSSION</b>	<b>61</b>
5.1	Introduction	61
5.2	Measurement of Calcination Temperature Range for Removing PVP	62
5.3	Formation of Crystalline Metal (Ni, Co, Mn, or Zn) Ferrite Nanoparticles	63
5.4	Investigation of Roles of PVP Concentration in Synthesis of Metal (Ni, Co, Mn or Zn) Ferrite Nanoparticles	66
5.4.1	XRD Patterns of Nickel Ferrite ( $\text{NiFe}_2\text{O}_4$ ) Nanoparticles	66
5.4.2	XRD Patterns of Cobalt Ferrite ( $\text{CoFe}_2\text{O}_4$ ) Nanoparticles	68
5.4.3	XRD Patterns of Manganese Ferrite ( $\text{MnFe}_2\text{O}_4$ ) Nanoparticles	70
5.4.4	XRD Patterns of Zinc Ferrite ( $\text{ZnFe}_2\text{O}_4$ ) Nanoparticles	72
5.4.5	TEM Images of Nickel Ferrite ( $\text{NiFe}_2\text{O}_4$ ) Nanoparticles	74
5.4.6	TEM Images of Cobalt Ferrite ( $\text{CoFe}_2\text{O}_4$ ) Nanoparticles	76
5.4.7	TEM Images of Manganese Ferrite ( $\text{MnFe}_2\text{O}_4$ ) Nanoparticles	77
5.4.8	TEM Images of Zinc Ferrite ( $\text{ZnFe}_2\text{O}_4$ ) Nanoparticles	79
5.4.9	FTIR Spectra of Nickel Ferrite ( $\text{NiFe}_2\text{O}_4$ ) Nanoparticles	80
5.4.10	FTIR Spectra of Cobalt Ferrite ( $\text{CoFe}_2\text{O}_4$ ) Nanoparticles	82
5.4.11	FTIR Spectra of Manganese Ferrite ( $\text{MnFe}_2\text{O}_4$ ) Nanoparticles	83
5.4.12	FTIR Spectra of Zinc Ferrite ( $\text{ZnFe}_2\text{O}_4$ ) Nanoparticles	85
5.5	Determine of the Optimum Time and Heating Rate of Calcination of Metal (Ni, Co, Mn or Zn) Ferrite Nanoparticles by XRD Technique	88
5.5.1	Optimum Heating Rate of Calcination of Nickel Ferrite Nanoparticles	89

5.5.2	Optimum Heating Rate of Calcination of Cobalt Ferrite Nanoparticles	90
5.5.3	Optimum Heating Rate of Calcination of Manganese Ferrite Nanoparticles	91
5.5.4	Optimum Heating Rate of Calcination of Zinc Ferrite Nanoparticles	92
5.6	Formation Mechanism of Bimetal ( $Ni_x Co_{1-x}$ ) Ferrite Nanoparticles	93
5.6.1	XRD Patterns of Nickel Cobalt Ferrite ( $Ni_x Co_{1-x} Fe_2O_4$ ) Nanoparticles	96
5.6.2	TEM Images of Nickel Cobalt Ferrite ( $Ni_x Co_{1-x} Fe_2O_4$ ) Nanoparticles	97
5.6.3	FTIR Spectra of Nickel Cobalt Ferrite ( $Ni_x Co_{1-x} Fe_2O_4$ ) Nanoparticles	99
5.7	Determine of the Optimum Time and Heating Rate of Calcination of Bimetal ( $Ni_x Co_{1-x}$ ) Ferrite Nanoparticles by XRD Technique	100
5.7.1	Optimum Heating Rate of Calcination of Nickel Cobalt Ferrite Nanoparticles	100
5.8	Crystallinity of Metal and Bimetal Ferrite Nanoparticles	102
5.8.1	XRD Patterns of Nickel Ferrite ( $NiFe_2O_4$ ) Nanoparticles	102
5.8.2	XRD Patterns of Cobalt Ferrite ( $CoFe_2O_4$ ) Nanoparticles	104
5.8.3	XRD Patterns of Manganese Ferrite ( $MnFe_2O_4$ ) Nanoparticles	106
5.8.4	XRD Patterns of Zinc Ferrite ( $ZnFe_2O_4$ ) Nanoparticles	108
5.8.5	XRD Patterns of Nickel Cobalt Ferrite ( $Ni_x Co_{1-x} Fe_2O_4$ ) Nanoparticles	110
5.9	Microscopic Morphology of Metal and Bimetal Ferrite Nanoparticles Performed by TEM Technique	112
5.9.1	TEM Images of Nickel Ferrite ( $NiFe_2O_4$ ) Nanoparticles	112
5.9.2	TEM Images of Cobalt Ferrite ( $CoFe_2O_4$ ) Nanoparticles	114
5.9.3	TEM images of manganese ferrite ( $MnFe_2O_4$ ) Nanoparticles	117
5.9.4	TEM images of zinc ferrite ( $ZnFe_2O_4$ ) nanoparticles	119
5.9.5	TEM images of Nickel Cobalt ferrite ( $Ni_x Co_{1-x} Fe_2O_4$ ) Nanoparticles	121
5.10	Calcination Temperature for Removing PVP from Metal and Bimetal Ferrite Nanoparticles	123
5.10.1	FTIR Spectra of Nickel Ferrite ( $NiF_2O_4$ ) Nanoparticles	124
5.10.2	FTIR Spectra of Cobalt Ferrite ( $CoFe_2O_4$ ) Nanoparticles	126
5.10.3	FTIR Spectra of Manganese Ferrite ( $MnFe_2O_4$ ) Nanoparticles	129
5.10.4	FTIR Spectra of Zinc Ferrite ( $ZnFe_2O_4$ ) Nanoparticles	132
5.10.5	FTIR Spectra of Nickel Cobalt Ferrite ( $Ni_x Co_{1-x} Fe_2O_4$ ) Nanoparticles	135

5.11	Microscopic Morphology of Metal and Bimetal Ferrite Nanoparticles Performed by SEM Technique	138
5.11.1	SEM Images of Nickel Ferrite ( $\text{NiFe}_2\text{O}_4$ ) Nanoparticles	138
5.11.2	SEM Images of Cobalt Ferrite ( $\text{CoFe}_2\text{O}_4$ ) Nanoparticles	139
5.11.3	SEM Images of Manganese Ferrite ( $\text{MnFe}_2\text{O}_4$ ) Nanoparticles	140
5.11.4	SEM Images of Zinc Ferrite ( $\text{ZnFe}_2\text{O}_4$ ) Nanoparticles	142
5.11.5	SEM Images of Nickel Cobalt Ferrite ( $\text{Ni}_x \text{Co}_{1-x} \text{Fe}_2\text{O}_4$ ) Nanoparticles	143
5.12	Summary of Optimization in Thermal Treatment Method	145
5.13	Magnetic Properties of Metal Ferrite Nanoparticles	146
5.13.1	VSM Measurements on Nickel Ferrite Nanoparticles	146
5.13.1.1	Variation of Saturation Magnetization with Calcinations Temperature in Nickel Ferrite Nanoparticle	146
5.13.1.2	Variation of Saturation Magnetization and Coercivity Field with Particle Size in Nickel Ferrite Nanoparticle	148
5.13.2	VSM Measurements on Cobalt Ferrite Nanoparticles	151
5.13.2.1	Variation of Saturation Magnetization with Temperature Calcinations in Cobalt Ferrite Nanoparticles	151
5.13.2.2	Variation of Saturation Magnetization, Coercivity Field, Remanent Magnetization and Remanence Ratio with Particle Size of Cobalt Ferrite Nanoparticles	154
5.13.3	VSM Measurements on Manganese Ferrite Nanoparticles	157
5.13.3.1	Variation of Saturation Magnetization with Calcination Temperature and Particle Size in Manganese Ferrite Nanopaticles	157
5.13.4	VSM Measurements on Zinc Ferrite Nanoparticles	160
5.13.4.1	Variation of Saturation Magnetization with Calcinations Temperature and Particle Size in Zinc Ferrite Nanoparticles	160
5.13.5	VSM Measurements on Nickel Cobalt Ferrite Nanoparticles	163
5.13.5.1	Variation of Saturation Magnetization with Temperature Calcinations in Nickel Cobalt Ferrite Nanopaticles	163
5.13.5.2	Variation of Saturation Magnetization, Coercivity Field, Remanent Magnetization and Remanence Ratio with Particle Size of Nickel Cobalt Ferrite Nanoparticles	165
5.13.6	EPR Measurements on Nickel Ferrite Nanoparticles	167

5.13.7	EPR Measurements on Cobalt Ferrite Nanoparticles	168
5.13.8	EPR Measurements on Manganese Ferrite Nanoparticles	169
5.13.8.1	Variation of Peak-to-Peak Line Width ( $\Delta H_{pp}$ ), Resonant Magnetic Field ( $H_r$ ), and g-factor with Calcination Temperature and Particles Size in Manganese Ferrite Nanoparticles	170
5.13.9	EPR Measurements on Zinc Ferrite Nanoparticles	171
5.13.9.1	Variation of Peak-to-Peak Line Width ( $\Delta H_{pp}$ ), Resonant Magnetic Field ( $H_r$ ), and g-factor with Calcination Temperature and Particles Size in Zinc Ferrite Nanoparticles	172
5.13.10	EPR Measurements on Nickel Cobalt Ferrite Nanoparticles	173
5.14	An Investigation on Magnetic Properties of Spinel Metal Ferrite Nanoparticles and their Preparation Methods	173
<b>6</b>	<b>CONCLUSION</b>	175
<b>REFERENCES</b>		178
<b>BIODATA OF STUDENT</b>		191
<b>LIST OF PUBLICATIONS</b>		192
<b>LIST OF PROCEEDING</b>		193
<b>LIST OF ACCEPTED</b>		193
<b>LIST OF SUBMITTED</b>		193
<b>LIST OF INTERNATIONAL CONFERENCES</b>		194